applied sciences

MDPI

Article

Mechanical Connectors to Enhance the Interfacial Debonding of Concrete Overlays

Rubén-Daniel López-Carreño [1], Sergio Carrascón [2], Antonio Aguado [1] and Pablo Pujadas [3,*]

[1] Department of Civil and Environmental, Universitat Politècnica de Catalunya (UPC-Barcelona Tech), Escola Tècnica Superior d'Enginyers de Camins Canals i Ports de Barcelona (ETSECCPB), Carrer de Jordi Girona, 1, 08034 Barcelona, Spain; rubenlc@gmail.com (R.-D.L.-C.); Antonio.aguado@upc.edu (A.A.)

[2] Instituto Español del Cemento y sus Aplicaciones (IECA), C/José Abascal, 53–1º, 28003 Madrid, Spain; scarrascon@ieca.es

[3] Department of Project and Construction Engineering, Universitat Politècnica de Catalunya (UPC-Barcelona Tech), Escola Tècnica Superior d'Enginyers Industrials de Barcelona (ETSEIB), Av. Diagonal, 647, 08028 Barcelona, Spain

* Correspondence: pablo.pujadas@upc.edu

Received: 17 April 2020; Accepted: 30 May 2020; Published: 3 June 2020

Abstract: Concrete bonded whitetoppings and overlays usually fail due to a loss of bond between the layers as a consequence of direct actions (traffic loads) or indirect actions (temperature differences or shrinkage in the layers). These actions generate stresses in the interface that may exceed the strength capacity of the union between layers. This paper proposed an innovative solution for this problem that consisted of placing mechanical connectors in the overlay interfaces to provide them with post-cracking strength and maintaining the monolithic response of the pavement. Three experimental programs on real-scale pavements with two types of mechanical connectors were studied under heavy traffic in terms of structural performance. Findings reveal that this technique might be an excellent solution to the problem of interfacial debonding.

Keywords: whitetopping; concrete overlay; pavements; debonding; post-cracking strength; screws-connectors

1. Introduction

Pavements are basic infrastructure, on intercities roads (highways, roads, among others) and in the urban environment. The interventions in them, both new construction and rehabilitation and/or strengthening, have an impact on economic, environmental, and social aspects, i.e., on its sustainability, thereby requiring an evaluation of the sustainability of these interventions [1,2].

Whitetoppings and overlays are pavement restoration techniques which consist of extending a Portland cement concrete layer over either an existing asphalt concrete (whitetoppings) or a Portland cement concrete (overlays). Both techniques can be cost-effective, rapidly constructed, and sustainable solutions compared to full pavement reconstruction [3].

The bond between the new concrete layer and the original pavement plays a key role in the structural response. When layers are bonded, the pavement resists in a monolithic manner and stresses in the materials due to external loads or indirect actions are diminished. Consequently, providing a proper bond allows the design of thinner overlays [4].

In recent decades, many studies were carried out to understand the mechanisms of bonding and debonding [5–13] and to bring recommendations for the maximization of the interfacial strength between layers in the whitetopping and overlays [8,14–16]. Moreover, some technical reports that give guidelines to select interfacial treatments and good construction practices were also published [4,15,17].

Nevertheless, in service situations, debonding is a very common problem that arises even when appropriate design and construction methods are used [18]. This tends to cause a premature failure before reaching the design life because the increment on stresses in the pavement layers. Therefore, the development of techniques and mechanisms that ensure a monolithic behaviour of the layers after losing their adherence is of great interest.

Techniques or mechanisms that guarantee post-cracking strength to the interface might help to eliminate the problem of loss of adhesion, as well as to dispense with adherence treatments at the interfaces. These would suppose a new approach in the conception of Portland cement concrete overlays in which interfacial debonding is admissible.

The objective of the present paper is to study the use of mechanical connectors for sewing the interface of Portland cement overlays subjected to heavy risk of interfacial cracking. Initially, mechanisms of debonding are described along with some of the most common practices to minimize the risk of interfacial cracking. After that, pure tensile interfacial strength is studied in a whitetopping with screw anchors on the interface. Finally, two real-size concrete overlays are presented and subsequently analyzed under heavy traffic loads.

2. Debonding Mechanisms and Reduction of Debonding Risk

The debonding of the whitetopping and overlays occurs mainly due to excessive interfacial stresses caused by direct and indirect loads. Direct loads are (1) vertical and (2) horizontal traffic loads while indirect ones are generated by (3) the autogenous shrinkage of the new concrete layer and (4) thermal and (5) moisture (drying shrinkage) exchanges with the environment [7]. All of them may simultaneously act in a real situation, thereby increasing the risk of interfacial debonding.

Table 1 shows the mechanisms of debonding classified by the type of loads and the typology of interfacial stresses. Vertical traffic loads (vehicle weight) generate normal interfacial stresses ($\sigma_{tr,v}$) that emerge near joints, cracks, or edges [8]. Owing to slab discontinuities, top and bottom layers are unable to deform jointly, and consequently $\sigma_{tr,v}$ emerges in the interface. These stresses increase when load transmission between adjacent slabs is poor and are also the leading cause of premature failure in whitetoppings [10,12].

Horizontal traffic loads (braking, acceleration, and centrifugal forces of vehicles) are applied by the wheel on the surface of the pavement. They make the slab tend to slip, so shear stresses ($\tau_{tr,h}$) appear in the opposite direction to avoid slippage. The magnitude of these stresses might be a major cause of interfacial failure [5,9,11,13].

On the other hand, thermal exchange, drying shrinkage, and autogenous shrinkage generate length changes that are translated into both normal and shear stresses [18–23]. In general, length changes are non-linear, so their effects may be decomposed into uniform and non-uniform components.

The uniform component may be understood as a rough simplification that helps to understand the debonding mechanisms. It generates shear ($\tau_{lc,u}$) stresses at the edge of overlay discontinuities to make deformations compatible. Concomitantly, normal tensile stresses ($\sigma_{lc,u}$) also arise close to the discontinuities due to the peeling moment generated by $\tau_{lc,u}$ and its eccentricity to the interface [7].

Finally, non-uniform length changes are related to curling and warping of overlay slabs. Upward and downward curvatures of concrete slabs induce normal tensile stresses ($\sigma_{lc,nu}$) to the interface due to the restraint produced by its adhesion to the original pavement. Sometimes, the magnitude of $\sigma_{lc,nu}$ is not negligible, as it can cause premature cracking of the interface [6].

It is possible to optimize the overlay design to reduce the stresses in the interface, enhance the adherence between layers, and to reduce the risk of interfacial debonding. The attributes to be optimized are the five cornerstones of design: (1) thickness of the concrete layer, (2) slabs size, (3) joint properties, (4) interfacial treatment, and (5) concrete mixture [15].

Table 1. Mechanism of interfacial debonding due to direct and indirect loads.

Load	Stresses	Mechanisms
Traffic (Vertical)	Normal	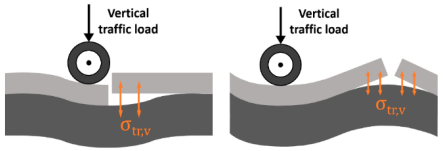
Traffic (Horizontal)	Shear	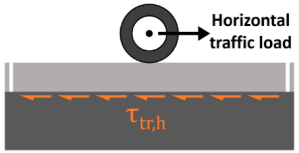
Thermal exchange/Drying shrinkage/Autogenous shrinkage	Shear (due to uniform component)	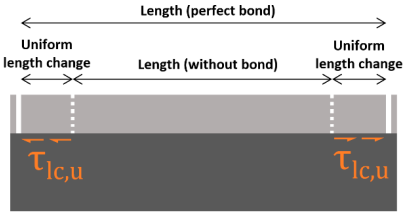
	Normal (peeling due to uniform length change)	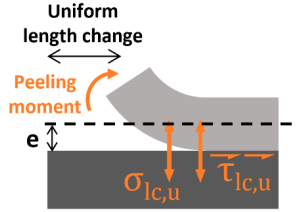
	Normal (due to non-uniform length change)	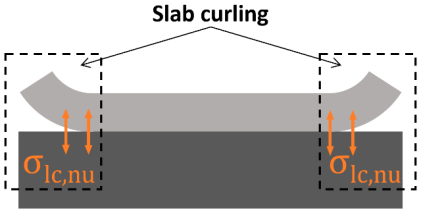

Doubling the thickness of the overlay might reduce normal tensile stresses in the interface due to vertical loads about 40 to 60% [12] and also decrease shear stresses due to horizontal traffic loads by about 24% [13]. Nevertheless, increasing the thickness increases the normal peeling stresses due to uniform length changes. This is due to the higher eccentricity of the interfacial shear stresses to the half the thickness of the overlay [7]. However, thicker overlays suffer shorter interfacial cracking lengths when subjected to drying shrinkage and temperature gradients due to the beneficial effect of self-weight forces [24].

The size of slabs may govern the failure mode of bonded whitetoppings on asphalt pavements [18,25,26]. Smaller slabs make it difficult to keep wheel paths away from joints, thereby incrementing the risk of flexural debonding due to vertical traffic loads [27]. Moreover, bigger slabs can rest a higher number of wheels on them, which increases shear stresses in the interface due to horizontal traffic loads [13]. Since stresses produced by uniform length changes are concentrated on the vicinity of discontinuities, size has no significant impact on them [28–30]. Nevertheless, interfacial stresses due to non-uniform length changes and subsequent curling and warping are lower in shorter slabs [31].

Joint properties determine load transfer between adjacent slabs and water penetration towards the interface. Load transfer between two adjacent slabs [32] is produced by both the effect of aggregate interlocking and continuity of the bottom layer of the pavement [10,33]. Fibers also contribute to improving the load transmission by limiting joint and cracks opening and generating a dowel bar effect [34]. Proper load transfer reduces the magnitude of normal debonding stress on the unloaded slab [10].

Water penetration towards the interface through the joints should be avoided because it might reduce interfacial bond strength. In addition, in the case of whitetoppings, the impact of water is more drastic since it can cause asphalt stripping and raveling [35]. To avoid this, joints must be sealed with hot-poured asphalt sealant and the use of backer rod should be avoided [15].

Interfacial treatment plays a crucial role in the mechanisms of interfacial debonding since the magnitude of the interfacial strength depends on it [36]. The most frequently used treatments relate to increasing the roughness of the interface, either by milling (for whitetoppings) or by shotblasting (for overlays) [15]. At the laboratory level, interface grooving has also shown good behavior [16]. Bonding agents should be employed very carefully because their coefficient of thermal expansion is usually very different from that of concrete [14] and weak planes might be generated at the interface [8].

Finally, the concrete mix also influences the mechanisms of both bond strength and stresses in the interface since compounds regulate the mechanical and physico-chemical properties of the overlay. For instance, high-performance concrete might not require additional treatment to the interface [37], the addition of fibers could also improve the adherence [38–40] and reduce the deterioration of joints and cracks [41]. Meanwhile, stronger aggregates and greater aggregate top size can also increase the load transfer in joints [32].

To reduce stresses produced by vertical and horizontal traffic loads, increasing the elastic modulus would be desirable [13,42]. In case of stresses due to variations in length, the mix can be optimized for reducing differential deformations between layers due to temperature, drying shrinkage, and autogenous shrinkage. Although the phenomena behind these change lengths are complex and involve many variables, a careful selection of as materials, mix proportion, pavement geometry, or degree of restraint can help in their minimization.

3. Mechanical Connectors to Enhance the Interface of Concrete Overlays

3.1. Design of the Connection between Layers

To maintain the monolithic structural behavior of concrete overlays after interfacial cracking, we propose to place mechanical connectors in their interfaces. If the connection is designed correctly,

pavement layers might remain working together after debonding, thereby preserving the expected service life of the restored pavement.

The working principle of connectors is analogous to that of steel rebars and fibers in concrete. Their stress resistance starts when the interface cracks and the load carried by the connectors increases, depending on the crack width [8]. In the design phase, the connection has to provide enough strength to resist the interfacial forces while local failure must be avoided in both the pavement layer and the connectors.

Model Code 2010 [43] provides Equation (1) to design mechanical connections subjected to fatigue or dynamic loads when the interfacial adhesive bond cannot be guaranteed. This equation considers that the strength of the interface between old and new concretes (τ_{Rd}) depends on (i) the aggregate interlocking, (ii) the shear-friction mechanism, and (iii) the bending resistance of connectors perpendicular to the joint (dowel action). Moreover, the value of τ_{Rd} (in MPa) is bounded from above by the product of a coefficient for the strength of the compression strut (β_c), a reduction factor for the strength of the diagonal strut ($\nu = 0.55 \cdot (30/f_{ck})^{1/3} \leq 0.55$), and the design value of concrete compressive strength of the weakest layer (f_{cd}).

The shear resistance due to interlocking is considered using a coefficient for aggregate interlocking (c_r) and the characteristic compressive strength of concrete (f_{ck}). The shear-friction strength is defined by a friction coefficient (μ), the compressive stress in the joint due to external normal forces (σ_n), an interaction coefficient for tensile force activated in the connectors (κ_1), the ratio ρ of the reinforcing steel crossing the interface ($\rho = A_s/A_c$; where A_s is the steel cross-section and A_c the concrete area where shear stresses occur), and its design yield strength (f_{yd}). Finally, dowel-action strength of the connectors is estimated in terms of ρ, f_{yd}, f_{cd} and an interaction coefficient for flexural resistance of the connector (κ_2).

$$\tau_{Rd} = 0.4 \cdot \left[c_r \cdot f_{ck}^{1/3} + \mu \cdot \left(\sigma_n + \kappa_1 \cdot \rho \cdot f_{yd} \right) + \kappa_2 \cdot \rho \cdot \sqrt{f_{yd} \cdot f_{cd}} \right] \leq 0.4 \cdot \beta_c \cdot \nu \cdot f_{cd} \quad (1)$$

Table 2 shows the values of the coefficients c_r, μ, κ_1, κ_2 and β_c in terms of the roughness (R_t) of the interface according to Model Code 2010. The value of R_t can be experimentally obtained with the sand path method [44]. Note that smoother surfaces have lower c_r, μ and κ_1 values (reduced interlocking and shear-friction strengths) and bigger κ_2 (high dowel-action strengths in the connectors).

Table 2. Coefficients c_r, μ, κ_1, κ_2 and β_c in terms of interfacial roughness according to Model Code 2010.

Surface Roughness	c_r	κ_1	κ_2	β_c	μ	
					$f_{ck} \geq 20$	$f_{ck} \geq 35$
Very Rough (e.g., high pressure water blasted, indented)—$R_t \geq 3.0$ mm	0.2	0.5	0.9	0.5	0.8	1.0
Rough (e.g., sand blasted, high pressure water blasted, etc.)—$R_t \geq 1.5$ mm	0.1	0.5	0.9	0.5	0.7	
Smooth (e.g., untreated, slightly roughened.)—$R_t < 1.5$ mm	0	0.5	1.1	0.4	0.6	
Very Smooth (e.g., cast against steel formwork)—R_t not measurable	0	0	1.5	0.3	0.5	

On the other hand, Figure 1 depicts the most relevant failure modes of anchors that must be avoided according to Model Code 2010 [43]. These are classified as steel fracture, concrete failure, concrete splitting, bond failure and blow-out. The main origins of these failures modes are insufficient steel strength and anchor transversal area, low concrete strength, and very little distance to borders, corners, and between anchors. Providing the ultimate limit states (ULS) design criteria for all these failure modes would require an extensive explanation which is not the purpose of this work. Nevertheless, accurate information and details on ULS requirements may be found in Reference [45].

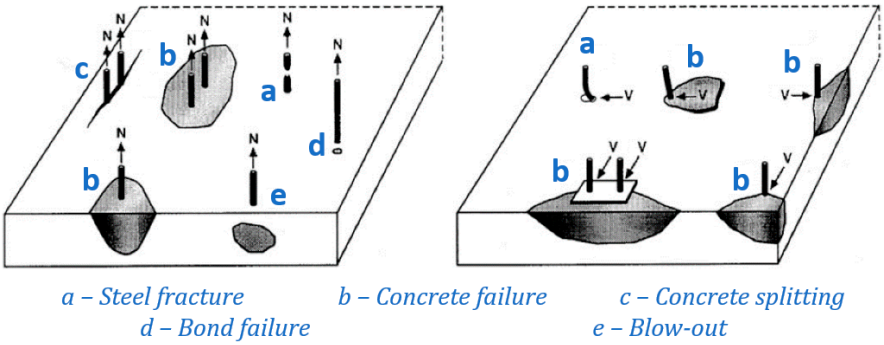

Figure 1. The failure mode of anchors (Source: Model Code 2010).

3.2. Mechanical Connectors Analyzed

In this work, two types of mechanical connectors to sew the interfaces of concrete overlays were analyzed. The first one corresponded to a hexagonal-head galvanized-steel screw commonly used for fastening applications in cracked and uncracked concrete. Its appearance and main characteristics are shown in Figure 2a and Table 3, respectively. A similar screw was studied in Reference [46] for strengthened beams. This element can be placed quickly (less than 30 s per piece) and is designed to generate low expansion forces. That makes it especially suitable to reduce the traffic opening time and minimize the damage in the bottom layer during its placement.

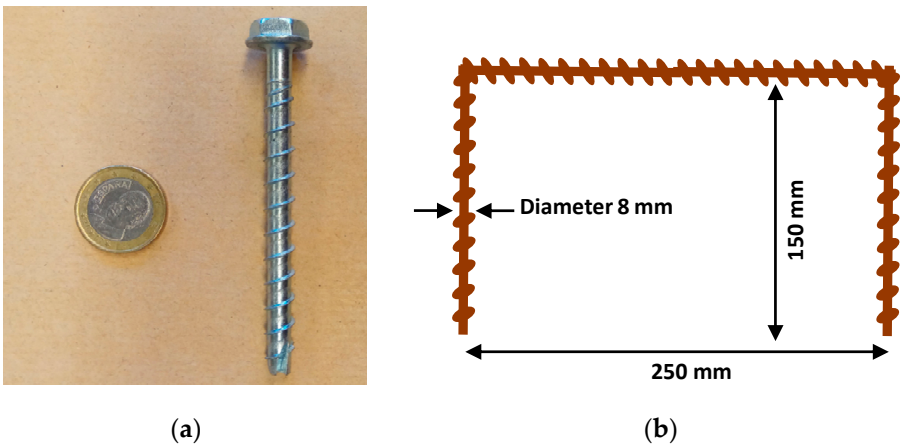

Figure 2. Mechanical connectors: (**a**) Screw, (**b**) ∏-shaped bended rebar.

Table 3. Characteristics of the screw anchors.

Property	Unit	Value
Height	(mm)	80
Outer diameter of thread	(mm)	7.85
Core diameter	(mm)	5.85
Nominal tensile strength	(MPa)	930
Stressed cross-section	(mm^2)	26.9

Figure 3a represents the forces acting in the screw anchor when the interface is subjected to an external tensile load. Analogous to the resistance mechanism of a foundation pile, the screw resists transmitting both friction forces to the original pavement layer and anchorage forces to the reinforcement layer. The resultant of the tensile force that loads the transversal area of the core of the screw is equal to the external tensile force applied on the interface.

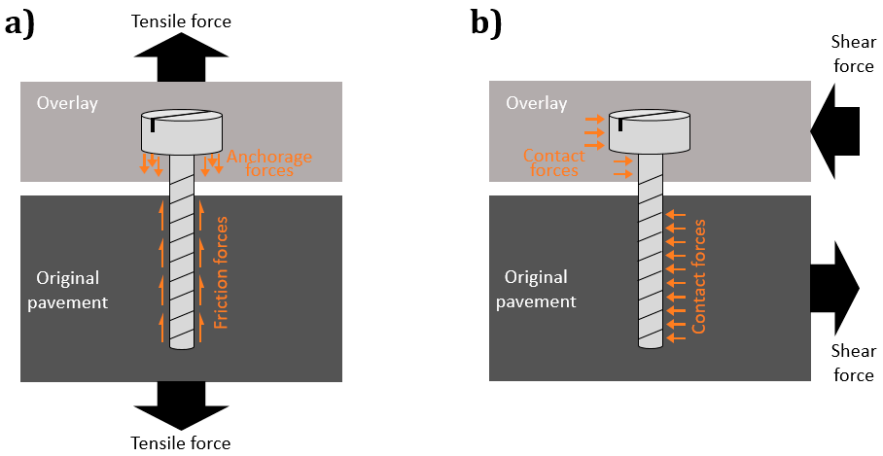

Figure 3. Mechanical behavior of a screw anchor under tensile (**a**) and shear (**b**) stresses.

On the other hand, Figure 3b schematizes the same interface but subjected to a horizontal shear force. In this case, the screw is capable of withstanding the loads by transferring contact forces whose resultants are of the same magnitude and direction opposite to that of the applied ones. The shear stresses that appear in the cross-section of the screw at the interface compensate for these loads.

The second connector was a ∏-shaped bended rebar 8 mm in diameter, 250 mm length, 150 mm height, 50.2 mm^2 cross-section, and 500 MPa nominal tensile strength (see Figure 2b). These bent rebars were placed in the most damaged zones of bonded whitetopping on asphalt concrete which required full-depth reconstructions. These reconstructions consisted of a bi-layer concrete pavement where the bottom asphalt was fully replaced by lean concrete and the top layer corresponded to an overlay. These rebars were selected because of their availability, their low cost, and the possibility to put them in the fresh lean concrete.

4. Experimental Validation

4.1. Pull-Off Behavior of Whitetopping Interfaces with Screw Anchors

A real-scale whitetopping was constructed and pull-off tests [47,48] were performed to study the installation of the screws and their influence on the mechanical behavior of an overlay interface. This test was selected because it is one of the most widely used methods to evaluate the bond between layers [37].

As Figure 4 shows, the whitetopping consisted of a 32.4 m^2 and 10 cm thick overlay on an asphalt concrete pavement in good condition and without slope. The whitetopping was formed by 4 slabs (slabs 1.a, 1.b, 2 and 3) of 1.80 m width, length between 2.60 and 6.00 m, and constructed without joints. A total of 110 screw anchors were installed on the interface of slabs 1.a and 1.b at a distance of 15 and 45 cm from the borders and spacings of 30 and 25 cm, respectively.

As seen in Figure 5a, the installation of the screws was performed by drilling a hole 5 cm deep and then placing and tightening the screw with a manual impact screwdriver. The 4 cm of the extreme of the screw core was inserted into the asphalt pavement while the rest of the core and the head were embedded into the concrete overlay (Figure 5b). The installation time of each screw was less than 30 s. The process of drilling, placing, and tightening was done by the same operators who later constructed the overlay.

About 15 min after placing the screw anchors in the interfaces of slabs 1.a and 1.b, the concrete layer of the whitetopping was constructed. For this, fixed formworks were placed, and subsequently, the surface of the asphalt was cleaned with water. After that, the concrete was poured onto the wet asphalt surface visually ensuring a similar moisture content in the areas where the pull-off test would be performed, i.e., the borders of slabs 1.a and 1.b and the entire surface of slabs 2 and 3 (Figure 6a).

Weather conditions during the placement of the overlay were cold (temperature at about 10 °C) and wet ambient without rainfall episodes. The compaction and levelling of the concrete were done using a vibrating screed (Figure 6b). The presence of screws did not interfere with these tasks.

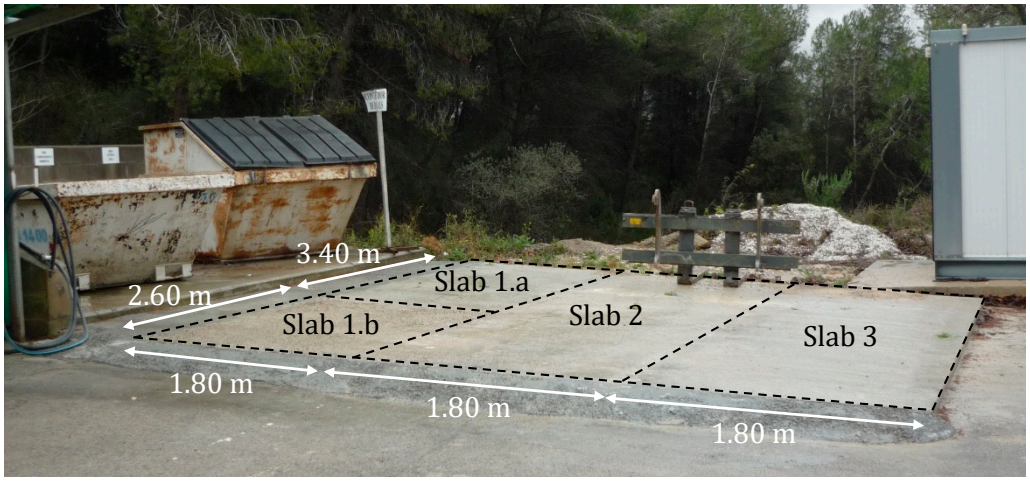

Figure 4. Appearance of the whitetopping.

(**a**) (**b**)

Figure 5. Screw anchor: installation (**a**) and appearance after installation (**b**).

Figure 6. Construction of the whitetopping: concrete pouring (**a**) and compaction (**b**).

Table 4 shows the mixes of the two concretes used to construct the whitetopping and their compressive strength at 24 h of age (measured according to [49]). A plain concrete without fibers was used for slabs 1.a and 3. For slabs 1.b and 2, the mix contained 3.0 kg/m^3 of 30 mm long polyolefin

fibers. Both mixes had a high content (500 kg/m^3) of CEM I 52.5 R cement with rapid development of mechanical properties, that allowed reaching strengths of about 50 MPa in 24 h.

Table 4. Concrete mixes of the whitetopping.

Materials (kg/m^3)	Slabs 1.a and 3	Slabs 1.b and 2
CEM I 52.5R cement	500	500
Limestone sand 0/4 mm	550	550
Silica sand 0/4 mm	220	220
Limestone sand 6/12 mm	975	975
Water	160	180
Superplasticizer	10	10
Polyolefin fibers	-	3.0
Compressive strength at 24 h (MPa)	54.0	47.7

The pull-off tests to measure the tensile strength of the interfaces were performed on 7 points after 135 days. As observed in Figure 7a, the tests were carried out on 100 mm diameter cores drilled to the bottom layer of asphalt. Threaded rods were attached to drilled holes in the top side of the cores using an epoxy resin. After that, the rods were pulled using an anchor tester which indicated the maximum tensile force performed during the test with a nominal precision of ±2.5% (Figure 7b).

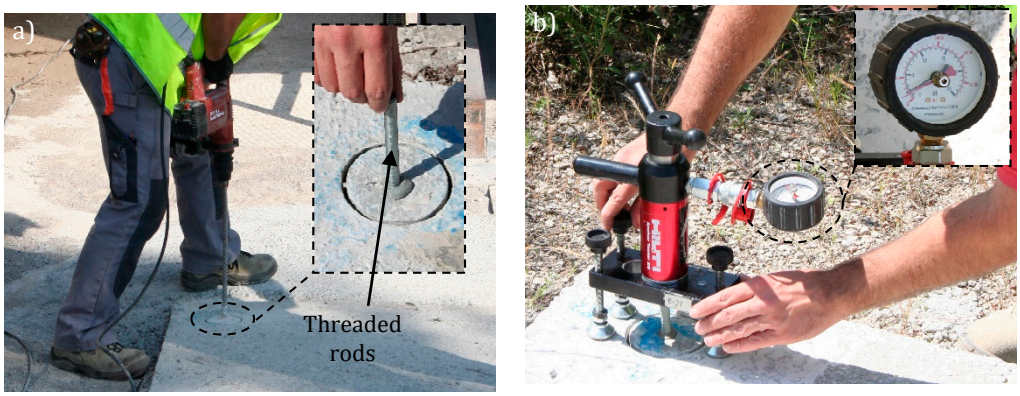

(**a**) (**b**)

Figure 7. Pull-off test: drilling and placing of threaded rods (**a**) and anchor tester (**b**).

Table 5 represents the results of the maximum forces ($P_{max,PO}$) and tensile stresses ($\sigma_{max,PO}$) reached by performing pull-off tests after 7 days of overlay hardening. All the results of tests were accepted according to the statistical Chauvenet's test for outliers [50]. The four cores without screws at the interface (slabs 2 and 3) failed through the interface between the concrete and the asphalt following the same failure mechanism. Since the screws only provide post-cracking strength, the results of these four tests were strictly provided by the bond strength between layers so they were representative of the pre-cracking interfacial strength.

The three cores with screw anchors in the interface (Slab 1.a) failed in two phases: a first one in which the cracking of the interface occurred and a second phase in which the applied load increased until reaching a maximum value. This maximum corresponded to the post-cracking strength provided by the screws given the tensile friction stresses between them and the asphalt. As the maximum load increased after cracking, the effect of the fibers on maximum tensile strength was negligible.

The presence of screws in the interface provided an average ultimate strength of 0.53 MPa (slab 1.a), which was 51.4% higher than the 0.35 MPa average strength obtained without them (slabs 2 and 2). In addition, the tests performed at the interfaces with screws showed less dispersion of results (variation coefficient of 6.53%) compared to the results of the interfaces without screws (variation coefficient of

51.80%). These results indicated, on the one hand, that screws provide tensile post-cracking strength to the interfaces which may be higher than their pre-cracking strength and, on the other hand, that the tensile behavior of the interface might be homogenized (less dispersion of results).

Table 5. Pull-off test results.

Slab	Code	Screw Anchors	$P_{max,PO}$ (kN)	$\sigma_{max,PO}$ (MPa)
1.a	SA-1	YES	4.0	0.51
	SA-2		4.0	0.51
	SA-3		4.5	0.57
2	NA-1	NO	1.0	0.13
	NA-2		2.5	0.32
	NA-3		3.0	0.38
3	NA-4	NO	4.5	0.57

4.2. Mechanical Behavior of Concrete Overlays with Screw Anchors under Heavy Traffic Loads

The pull-off tests demonstrated that the placement of screw anchors in the interface of the whitetoppings might be a suitable solution to enhance the tensile interfacial strength without a substantial increase in construction time. A 229.4 m long, 3.10 m width and 10 cm thick overlay was built (see Figure 8a) to assess that this technical solution was valid for the construction of real pavements. The pavement was located in a cement plant and closely placed to a cement clinker kiln, so the area was subjected to temperatures higher than its surroundings. The objective of this test was to determine if concrete overlays with screw anchors were capable of resisting a high flux of heavy-weight vehicles without structural damage.

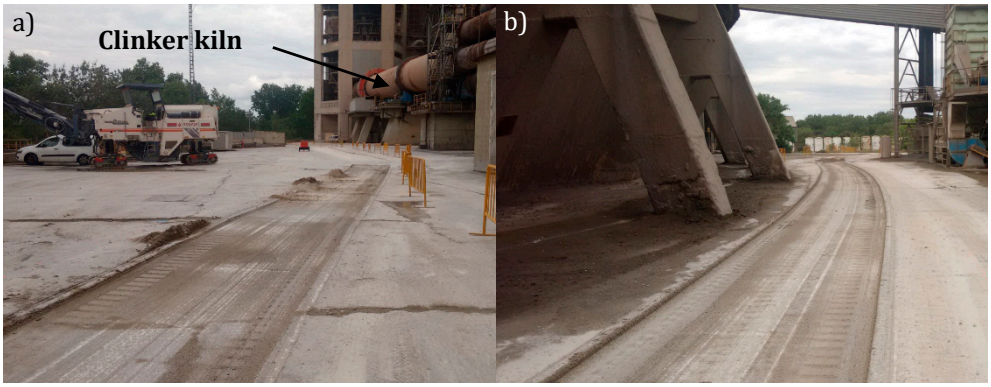

Figure 8. Original concrete pavement (**a**). The appearance of the cold-milled box (**b**).

The original pavement was cold-milled to leave a box with the width and thickness of the reinforcement (Figure 8b). Four rows of screws were arranged in the milled surface following the symmetrical scheme in Figure 9. Since normal and shear stresses due to direct and indirect loads mainly concentrate next to discontinuities, the double density of the screws were installed in the borders of the overlay.

As presented in Figure 10a, the 4 cm of the extreme of the screw core was inserted into the concrete to subsequently embed the remaining 4 cm and the head into the overlay. Then, 24 h after that, the concrete was poured and extended in a single day (without construction joints) using an asphalt paver (see Figure 10b) and then compacted with rollers. Joints were cut at a distance of 3.5 m. The total duration of building the test setup was two days.

Table 6 presents the mix of the concrete overlay. The amount of water was adapted to improve the extension and compaction processes. For the mechanical characterization, six cylindrical specimens (ϕ150 mm × 150 mm) and six beams (150 mm × 150 mm × 600 mm) were cast. After 28 days,

compression (f_c) and flexural ($f_{ct,fl}$) strength tests were carried out. Results of f_c ranged from 55.45 MPa to 60.36 MPa while the values of $f_{ct,fl}$ were between 5.62 MPa and 6.41 MPa.

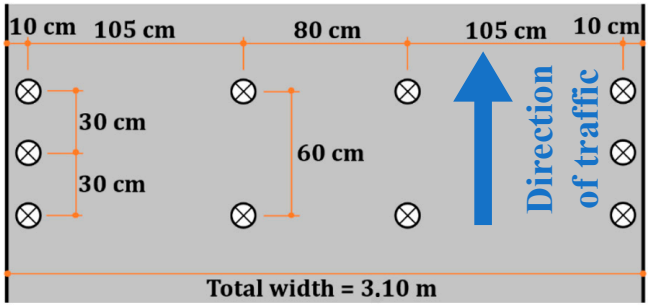

Figure 9. Arrangement of the screws.

(**a**) (**b**)

Figure 10. Screw anchors in the milled surface (**a**). Asphalt paver extending the concrete (**b**).

Table 6. Concrete mix of the overlay with screws in the interface.

Material	Content
CEM I 52.5 R	400 kg/m^3
Limestone sand 0/2 mm	515 kg/m^3
Limestone gravel 6/12 mm	1300 kg/m^3
Water	125 to 135 kg/m^3
Superplasticizer	2.4 L/m^3
Plastificizer	2.4 L/m^3

Two days after construction, a visual survey was made to analyze the presence of pavement damage. Since the opening to heavy traffic was made after 7 days, potential damage would be associated with the very early age behavior of concrete. As depicted in Figure 11a–c, transversal and longitudinal cracks appeared in most of the slabs, which could be explained by excessive shrinkage. It must be stated that during concrete hardening, many of the leading causes for shrinkage could have come together, i.e., a very high rate of concrete evaporation due to both high ambient temperature (above 25 °C) and direct solar radiation, the use of rapid-hardening cement in the concrete mix, an insufficient curing and/or an excessive distance between joints. Nevertheless, after three years of construction, no significant damage was noticed, so it could be affirmed that the overlay with screws performed adequately in terms of structural behavior under heavy traffic.

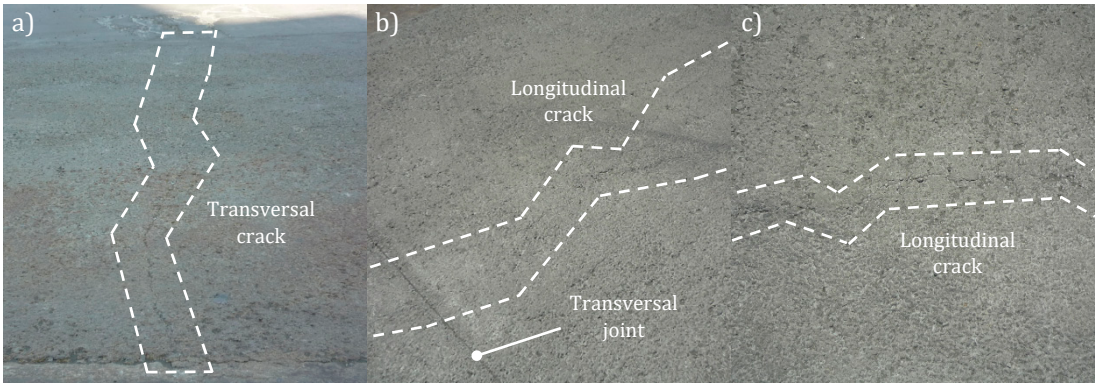

Figure 11. Shrinkage cracks: transversal (**a**), longitudinal (**b**) and detail (**c**).

4.3. Mechanical Behavior of Concrete Overlays with Bended Rebars

Pull-off and real-scale tests subjected to traffic loads showed that the use of screw anchors might be a proper constructive technique to reduce the risk of premature failure due to interfacial debonding. Having this in mind, a similar solution using ∏-shaped bended rebars was studied in the pavement restoration of four roundabouts placed on the N-II National Road at La Jonquera (Spain).

The original pavements of the roundabouts consisted of 31 cm thick asphalt concrete on 25 cm thick graded aggregate and were subjected to very heavy traffic (>4.000 trucks/day). The damage caused by the combination of traffic loads and continuous fuel spills made it necessary to replace the asphalt layer several times at different depths. The pavements of the four roundabouts were reconstructed to provide a permanent solution.

Two different structural solutions were proposed. The first one (WT) was a whitetopping in which 12 cm of the bituminous mix was replaced by Portland cement concrete, where the mix composition is shown in Table 7. The second solution (OL) was a full-depth reconstruction which consisted of two layers of Portland cement concrete with bent rebars in the interface. The bottom layer was lean concrete placed up to level −12 cm (same level as the asphalt of WT solution) while the top layer was the prolongation of the concrete of the WT. The WT was the general solution for the pavements while the OL was constructed in the most damaged areas of the four roundabouts.

Table 7. Concrete mix of the overlay.

Material	Content
CEM I 52.5 R (kg/m^3)	430
Aggregate 10/20 mm (kg/m^3)	750
Aggregate 4/12 mm (kg/m^3)	200
Aggregate 0/4 mm (kg/m^3)	900
Polyolefin fibers (kg/m^3)	4.0
Water (L/m^3)	155
Superplasticizer (L/m^3)	3.0
Water reducer (L/m^3)	5.0

Figure 12 shows the visual aspect of the pavement before restoration. The asphalt presented widespread and several damages due to fuel spills combined with traffic fatigue (bitumen loss, cracking, wheel path rutting, potholes, etc.). Visual inspection and load plate tests were performed on all four roundabouts to determine the most severely affected regions. Four areas were detected with an exceptionally low ballast coefficient (K_{60}), while for the rest of the pavement a Winkler coefficient of 391 MPa was assumed as a representative value.

The first construction activity was the cold-milling of the top 12 cm of asphalt concrete, leaving 30 to 50 cm wide unmilled strips on the outer and interior edges of the roundabouts. The asphalt of the

four areas with more damage was full-depth milled until the graded aggregate was visible, followed by replacement with C15 lean concrete (fc = 15 MPa at 28 days) up to a height of −12 cm concerning the initial surface level.

Figure 12. Previous pavement condition of the roundabouts.

As presented in Figure 13a, the ∏-shaped bended rebars were placed in the top surface of the C15 concrete protruding 50 mm above it. The protrusion height was defined to ensure more than twice the maximum aggregate size of the mix (20 mm) to avoid hollows after concrete vibration. An accuracy of ±10.0 mm was assumed for the rebars placement process. The rebars were arranged to form a grid of 25 cm × 25 cm so that the interface would become homogenously sewn in both the traffic and its perpendicular directions (see Figure 13b).

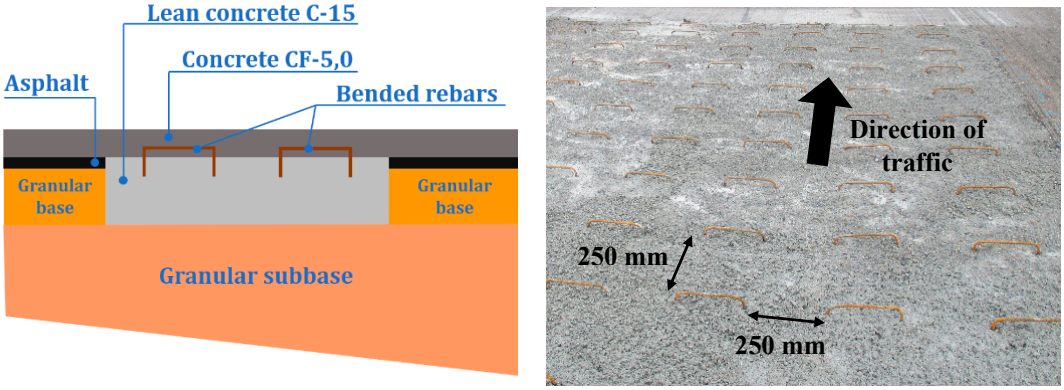

(**a**) (**b**)

Figure 13. Detail of mechanical connection between concretes (**a**). Arrangement of the bent rebars in the bottom concrete layer (**b**).

After that, the concrete of the 12 cm thick overlay was placed over the continuous surface formed by the milled asphalt and the C15 repairs. The concrete was a CF-5.0 type (see Table 7) with 4.0 kg/m^3 of short structural polyolefin fibers (12 mm in length), nominal flexural strength at 28 days of $f_{ct,fl}$

= 5.0 MPa, and slump of 7 to 10 cm in the Abrams cone. Quality control tests of CF-5.0 showed a $f_{ct,fl}$ = 5.0 MPa and f_c = 35.0 MPa were reached after 7 days.

As shown in Figure 14a,b, pouring, compacting, and finishing of the CF-5.0 is done using manual methods. Both radial and concentric slab joints were cut 6 to 12 h after placing the CF-5.0 overlay and subsequently sealed with materials resistant to diesel fuel. Radial joints were sealed with nitrile-butadiene rubber profile while concentric ones were filled with hot mastic asphalt.

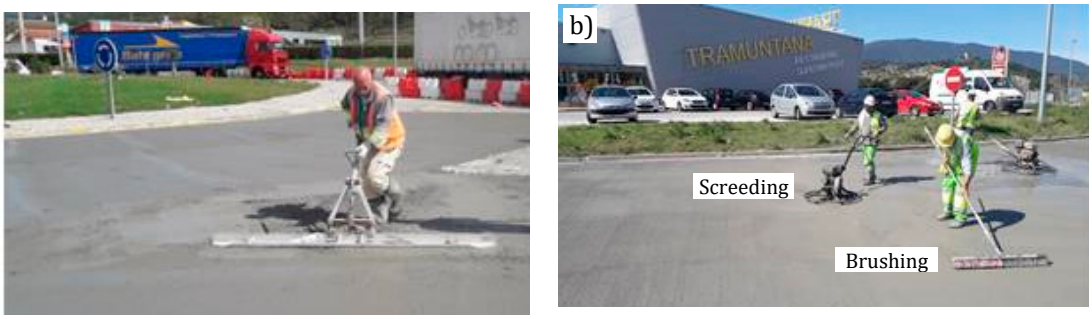

(**a**) (**b**)

Figure 14. Compaction of the overlay (**a**) and surface finishing (**b**).

Figure 15 shows the finished whitetopping of the roundabouts with open traffic. The time between construction and opening to traffic was between 7 and 15 days to ensure that at least 80% of $f_{c,f}$ = 5.0 MPa was achieved. Average depths measured with the sand patch test (UNE-EN 13036-1:2010) were larger than 1.10 mm, indicating that surface finishing was suitable even for speeds higher than 100 km/h.

Figure 15. The final appearance of the roundabouts.

Two years after construction, a visual survey was conducted to determine the existence of cracks and surface faults. The slabs corresponding to zones with full-depth reconstruction and bent rebars in the interface (OL) did not present cracks (see Figure 16a). Meanwhile, cracks appeared in some of the concrete slabs of the WT, which corresponded to about 10% of the total number of slabs of the pavement of the four roundabouts (see Figure 16b,c). Moreover, as Figure 16d shows, the transition between WT and OL was sometimes clearly observed at simple sight, since cracks in WT were not prolonged to the slabs of the OL solution.

The presence of cracks might be explained by the fact that the actual stiffness of the asphalt in the zones would be lower than that assumed in the overlay design. A more extensive campaign of load plate tests could help to determine the mechanical parameters of the asphalt more accurately. Nevertheless, as the stiffness of the asphalt reduces, the concrete overlay of the WT should be thicker, thereby increasing the global cost of the pavement restoration.

Considering the above, it can be stated that the structural performance of the OL solution was excellent and superior to that of the WT solution directly on the asphalt. Consequently, the use of

steel bended rebars at the interface of bi-layer concrete pavement is a feasible alternative for the reconstruction pavements subjected to the high flux of heavyweight vehicles.

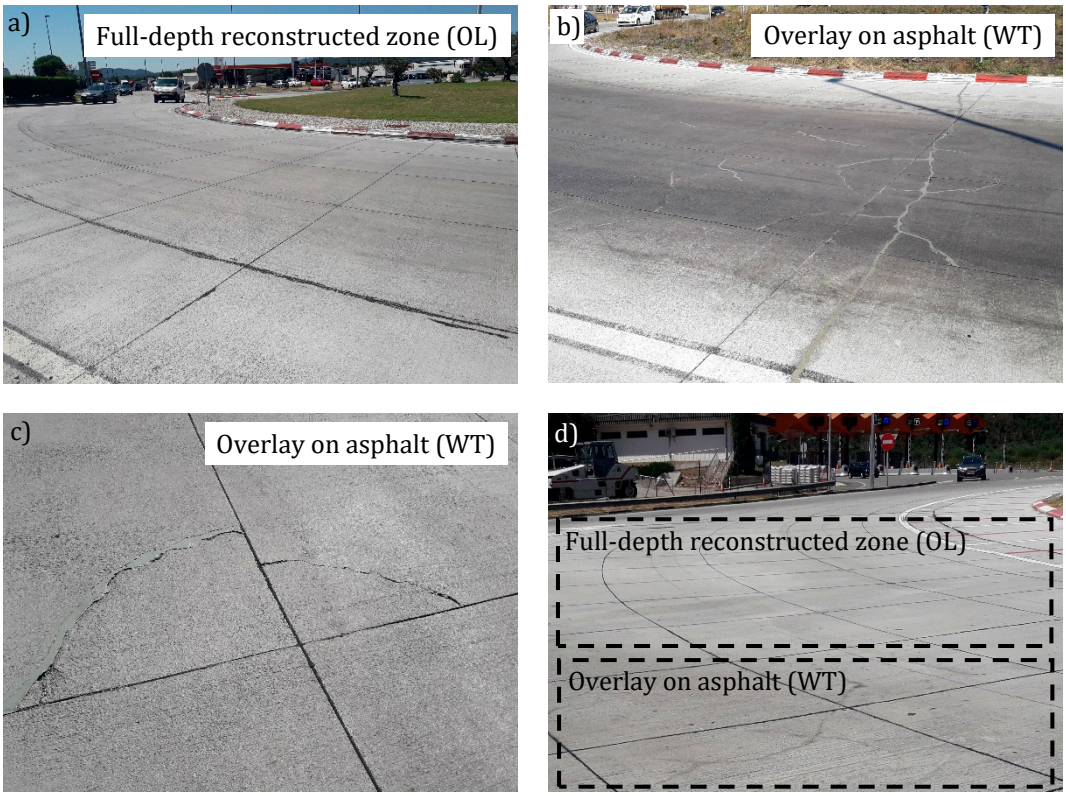

Figure 16. Roundabouts after two years: area with full-depth reconstruction (**a**), general view of cracks in the WT solution (**b**), detail of corner crack (**c**), and transition between WT and OL solutions (**d**).

5. Conclusions

In this work, the use of mechanical connectors is proposed for bringing post-cracking strength to interfaces of Portland cement concrete overlays for pavement applications. To this end, the mechanisms that may produce interfacial debonding and common practices to reduce the risk of debonding were presented. Two types of connectors (screws and bended rebars) were tested on two real-scale pavements to analyze the structural performance of overlays with the sewed interface. From this, the following conclusions are derived:

- The mechanical behavior of mechanicals connectors is analogous to that of steel rebars reinforcement and fibers in concrete. They begin to resist stresses just after the interface cracking and increase the resisted load when the crack opens. Thanks to this, the layers still work together after debonding thereby preventing excessive stress increments in the materials.
- Screw anchors are a fast-track suitable solution to provide residual post-cracking strength to the interface of concrete overlays on existing pavements. They can be installed with light tools by non-skilled operators, without significantly affecting the construction process and timing. Pull-off tests in bonded whitetoppings showed both an increment in average maximum tensile strength and a homogenization (reduction of dispersion) of the resistant behavior. The averages and coefficient of variations of maximum strength were 0.53 MPa and 6.53% in interfaces with screws and 0.35 MPa and 51.80% in interfaces without screws.
- After three years of very heavy traffic, the 229.4 m × 3.10 m × 0.10 m overlay with screw anchors in the interfaces performed correctly without developing structural cracks. In this case, damages only

appeared in the first hours due to excessive evaporation, insufficient curing and/or an excessive distance between joints.

- The use of bent rebars may be an excellent low-cost alternative for sewing the interface of bi-layer concrete pavements. The overlay of the four roundabouts presented higher structural performance in the areas with two layers of concrete and bended rebars than those with an asphalt bottom layer. After two years of traffic, about 10% the total of roundabouts slabs were cracked, none of them in regions with mechanical connectors in the interface.
- Portland cement overlays with mechanical connectors placed in their interface performed satisfactorily in structural terms after being subjected to a high flow of heavy vehicles. This constructive solution might be an opportunity to extend the use of overlays in situations where a high risk of interfacial debonding exists.

Author Contributions: Conceptualization, R.-D.L.-C., A.A and P.P.; methodology, R.-D.L.-C. and P.P.; validation, and formal analysis, R.-D.L.-C. and S.C.; investigation, R.-D.L.-C.; writing—original draft preparation, R.-D.L.-C.; writing—review and editing, P.P.; visualization, S.C. and A.A.; supervision, S.C., A.A and P.P.; project administration, P.P.; funding acquisition, A.A. All authors have read and agree to the published version of the manuscript.

Funding: This research was funded by Spanish Ministry of Economy and Competitiveness, grant number IPT-2012-0313-370000.

Acknowledgments: The authors would like to thank the Spanish Ministry of Economy and Competitiveness for the financial support provided by the project "Desarrollo de Mejores Rehabilitaciones Locales en Infraestructuras (MERLIN)" (Subprograma INNPACTO) IPT-2012-0313-370000. Ministerio de Economía y Competitividad (Spain). The first author also wishes to thank the Agència de Gestió d'Ajuts Universitaris i de Recerca of the Generalitat de Catalunya and the European Social Fund of the European Union for their financial support provided by the FI-DGR grant.

Conflicts of Interest: The authors declare no conflict of interest.

References

1. Aguado, A.; Gálvez, J.C.; Aguado-Renter, A.; Pujadas Álvarez, P.; Fernández-Ordoñez, D. Evaluación de la sostenibilidad de carreteras. *Carreteras* **2017**, *4*, 8–19.
2. Pujadas, P.; Cavalaro, S.H.P.; Aguado, A. MIVES multicriteria assessment of urban-pavement conditions: Application to a case study in Barcelona. *Road Mater. Pavement Des.* **2019**, 1–17. [CrossRef]
3. Torres, H.N.; Roesler, J.; Rasmussen, R.O.; Harrington, D. *Guide to the Design of Concrete Overlays Using Existing Methodologies*; IOWA State University, National Concrete Pavement Technology Center: Ames, IA, USA, 2012.
4. Rasmussen, R.O.; Rozycki, D.K. *Thin and Ultra-Thin Whitetopping—A Synthesis of Highway Practice NCHRP Synthesis*; Transportation Research Board: Washington, DC, USA, 2004; Volume 338.
5. Lau, C.M.; Fwa, T.F.; Paramasivam, P. Interface shear stress in overlaid concrete pavements. *J. Transp. Eng.* **1994**, *120*, 163–177. [CrossRef]
6. Mailvaganam, N.; Springfield, J.; Repette, W.; Taylor, D. Curling of concrete slabs on grade. *Constr. Technol. Update* **2000**, *44*, 1–6.
7. Granju, J.-L. Debonding of Thin Cement-Based Overlays. *J. Mater. Civil Eng.* **2001**, *13*, 114–120. [CrossRef]
8. Silfwerbrand, J.; Beushausen, H.; Courard, L. *"Bond." Bonded Cement-Based Material Overlays for the Repair, the Lining or the Strengthening of Slabs or Pavements*; Springer: Dordrecht, The Netherlands, 2011; pp. 51–79.
9. Eid, J. *Theoretische und Experimentelle Untersuchungen Dünner Betondecken auf Asphalt (Whitetopping)*; Lehrstuhl und Prüfamt für Verkehrswegebau: Munich, Germany, 2012.
10. Barman, M.; Vandenbossche, J.M.; Li, Z. Characterization of Load Transfer Behavior for Bonded Concrete Overlays on Asphalt. *Transp. Res. Rec. J. Transp. Res. Board* **2015**, *2524*, 143–151. [CrossRef]
11. Nguyen Dinh, N. Precast Ultra-Thin Whitetopping (PUTW) in Singapore and Its Application for Electrified Roadways. Ph.D. Thesis, Technische Universität München, Lehrstuhl und Prüfamt für Verkehrswegebau, München, Germany, 2016.
12. Barman, M.; Vandenbossche, J.M.; Li, Z. Influence of Interface Bond on the Performance of Bonded Concrete Overlays on Asphalt Pavements. *J. Transp. Eng. Part B Pavements* **2017**, *143*, 04017008. [CrossRef]

13. Kim, Y.K.; Lee, S.W. Numerical analysis of debonding mechanism in bonded concrete overlay according to horizontal traffic loading. *Constr. Build. Mater.* **2017**, *131*, 327–333. [CrossRef]
14. Roy, M.; Ray, I.; Davalos, J.F. High-performance fiber-reinforced concrete: Development and evaluation as a repairing material. *J. Mater. Civ. Eng.* **2013**, *26*, 04014074. [CrossRef]
15. Harrington, D.; Fick, G. *Guide to Concrete Overlays: Sustainable Stubs for Resurfacing and Rehabilitating Existing Pavements*, 3rd ed.; National Concrete Pavement Technology Center: Ames, IA, USA, 2014.
16. Jayakesh, K.; Suresha, S.N. Experimental investigation of interface treatment technique on interface shear bond fatigue behavior of Ultra-Thin Whitetopping. *Constr. Build. Mater.* **2018**, *161*, 489–500. [CrossRef]
17. Bissonnette, B.; Courard, L.; Fowler, D.W.; Granju, J.L. (Eds.) *Bonded Cement-Based Material Overlays for the Repair, the Lining or the Strengthening of Slabs or Pavements*; State-of-the-Art Report of the RILEM Technical Committee 193-RLS Series; Springer: Dordrecht, The Netherlands, 2011; p. 3.
18. Li, Z.; Vandenbossche, J.M. *Redefining the Failure Mode for Thin and Ultra-Thin Whitetopping with a 1.8- × 1.8-m (6- × 6-ft) Joint Spacing*; Transportation Research Board of the National Academics: Washington, DC, USA, 2013; pp. 133–144.
19. Beushausen, H.; Alexander, M.G. Failure mechanisms and tensile relaxation of bonded concrete overlays subjected to differential shrinkage. *Cem. Concr. Res.* **2006**, *36*, 1908–1914. [CrossRef]
20. Theiner, Y.; Hofstetter, G. Evaluation of the effects of drying shrinkage on the behavior of concrete structures strengthened by overlays. *Cem. Concr. Res.* **2012**, *42*, 1286–1297. [CrossRef]
21. Kim, M.O.; Bordelon, A. Numerical Study on the Cracking Behavior of Fiber-Reinforced Concrete Overlay Subjected to Temperature Loading. In *Cold Regions Engineering*; American Society of Civil Engineers: Reston, VA, USA, 2015; pp. 252–263.
22. Amidi, S.; Wang, J. Subcritical debonding of FRP-to-concrete bonded interface under synergistic effect of load, moisture, and temperature. *Mech. Mater.* **2016**, *92*, 80–93. [CrossRef]
23. Zhou, A.; Büyüköztürk, O.; Lau, D. Debonding of concrete-epoxy interface under the coupled effect of moisture and sustained load. *Cem. Concr. Compos.* **2017**, *80*, 287–297. [CrossRef]
24. Lange, D.; Shin, H.C. Early age stresses and debonding in bonded concrete overlays. *Transp. Res. Rec. J. Transp. Res. Board* **2001**, *1778*, 174–181. [CrossRef]
25. Barman, M.; Vandenbossche, J.M.; Mu, F.; Gatti, K. *Development of a Rational Mechanistic-Empirical Based Design Guide for Thin and Ultra-Thin Whitetopping*; Univ. of Pittsburgh: Pittsburgh, PA, USA, 2011.
26. Li, Z.; Vandenbossche, J.M.; Dufalla, N. Structural Model for Longitudinal Cracking in Bonded Whitetopping with a 1.83 m × 1.83 m Joint Spacing. *J. Transp. Eng. Part B Pavements* **2017**, *143*, 04017015. [CrossRef]
27. Burnham, T. MnROAD Lessons Learned: Thin and Ultra-Thin Concrete Overlays, Minnesota Department of Transportation, Office of Materials 9/26/2006, 2006. Available online: http://www.dot.state.mn.us/mnroad/reports/PDF%27s/whitetopping.pdf (accessed on 12 November 2018).
28. Jonasson, J.-E. *Computer Program for Non-Linear Computations in Concrete with Regard to Shrinkage, Creep, and Temperature*; CBI Report No. 7:77; Swedish Cement and Concrete Research Institute: Stockholm, Sweden, 1977; 161p. (In Swedish)
29. Silfwerbrand, J. *Differential Shrinkage in Composite Concrete Beams of Old Concrete and a New-Cast Concrete Overlay*; Bulletin No. 144; Department of Structural Mechanics and Engineering, Royal Institute of Technology: Stockholm, Sweden, 1986; 149p. (In Swedish)
30. Silfwerbrand, J. Differential shrinkage in normal and high strength concrete overlays. *Nord. Concr. Res.* **1996**, *19*, 55–68.
31. Chen, D.H.; Won, M.; Chen, X.; Zhou, W. Design improvements to enhance the performance of thin and ultra-thin concrete overlays in Texas. *Constr. Build. Mater.* **2016**, *116*, 1–14. [CrossRef]
32. Vandenbossche, J. Estimating potential aggregate interlock load transfer based on measurements of volumetric surface texture of fracture plane. *Transp. Res. Rec. J. Transp. Res. Board* **1999**, *1673*, 59–63. [CrossRef]
33. Vandenbossche, J.M.; Barman, M.; Nolan-Kremm, J. Surface Texture Measurements of Crack Surface to Establish Joint Shear Stiffness. *Transp. Res. Rec.* **2014**, *2441*, 13–19. [CrossRef]
34. Destrée, X.; Yao, Y.; Mobasher, B. Sequential cracking and their openings in steel-fiber-reinforced joint-free concrete slabs. *J. Mater. Civ. Eng.* **2015**, *28*, 04015158. [CrossRef]
35. Vandenbossche, J.M.; Barman, M. Bonded whitetopping overlay design considerations for prevention of reflection cracking, joint sealing, and the use of dowel bars. *Transp. Res. Rec.* **2010**, *2155*, 3–11. [CrossRef]

36. Mu, F.; Vandenbossche, J.M.; Janssen, D.J. Quantifying the mode I energy release rate for interface fracture of Portland cement concrete bonded to asphalt. In Proceedings of the American Concrete Institute Spring Convention, Minneapolis, MN, USA, 14–18 April 2013.
37. López-Carreño, R.D.; Pujadas, P.; Cavalaro, S.H.; Aguado, A. Bond strength of whitetoppings and bonded overlays constructed with self-compacting high-performance concrete. *Constr. Build. Mater.* **2017**, *153*, 835–845. [CrossRef]
38. Banthia, N.; Dubeau, S. Carbon and steel microfiber-reinforced cement-based composites for thin repairs. *J. Mater. Civ. Eng.* **1994**, *6*, 88–99. [CrossRef]
39. Zanotti, C.; Banthia, N.; Plizzari, G. A study of some factors affecting bond in cementitious fiber reinforced repairs. *Cem. Concr. Res.* **2014**, *63*, 117–126. [CrossRef]
40. Zanotti, C.; Rostagno, G.; Tingley, B. Further evidence of interfacial adhesive bond strength enhancement through fiber reinforcement in repairs. *Constr. Build. Mater.* **2018**, *160*, 775–785. [CrossRef]
41. Vandenbossche, J.; Fagerness, A. Performance, analysis, and repair of ultrathin and thin whitetopping at Minnesota road research facility. *Transp. Res. Rec. J. Transp. Res. Board* **2002**, *1809*, 191–198. [CrossRef]
42. Chabot, A.; Hun, M.; Hammoum, F. Mechanical analysis of a mixed mode debonding test for "composite" pavements. *Constr. Build. Mater.* **2013**, *40*, 1076–1087. [CrossRef]
43. *fib*-Fédération Internationale du Béton. *Model Code 2010*; Fédération Internationale du Béton: Lausanne, Switzerland, 2010.
44. *UNE-EN 13036-1:2010. Road and Airfield Surface Characteristics-Test Methods-Part 1: Measurement of Pavement Surface Macrotexture Depth Using a Volumetric Patch Technique*; AFNOR: Paris, France, 2010.
45. Engström, B. *Structural Connections for Precast Concrete Buildings*; International Federation of Structural Concrete: Lausanne, Switzerland, 2008.
46. Munger, F.; Wicke, M.; Jirsa, O.G. Connection of old concrete with new concrete-overlays. In *IABSE Symposium, Extending the Lifespan of Structures*; IABSE: Zurich, Switzerland, 1995; Volume 73, p. 2.
47. ASTM D4541-17. *Standard Test Method for Pull-Off Strength of Coatings Using Portable Adhesion Testers*; ASTM International: West Conshohocken, PA, USA, 2017.
48. Bonaldo, E.; Barros, J.A.; Lourenço, P.B. Bond characterization between concrete substrate and repairing SFRC using pull-off testing. *Int. J. Adhes. Adhes.* **2005**, *25*, 463–474. [CrossRef]
49. *UNE EN 12390-3:2009. Testing Hardened Concrete-Part 3: Compressive Strength of Test Specimens*; British Standard Institution: London, UK, 2009.
50. Taylor, J.R. *An Introduction to Error Analysis—The Study of Uncertainties in Physical Measurements*, 2nd ed.; University Science Books: Sausalito, CA, USA, 1997; p. 349.